HHS Public Access

Author manuscript

Photochem Photobiol. Author manuscript; available in PMC 2018 November 01.

Published in final edited form as:

Photochem Photobiol. 2017 November ; 93(6): 1502–1508. doi:10.1111/php.12805.

Effects of Combined Lysosomal and Mitochondrial Photodamage in a Non Small-Cell Lung Cancer Cell Line: the Role of Paraptosis

David Kessel[1,*] and **John J. Reiners Jr.**[1,2]

[1]Department of Pharmacology, Wayne State University School of Medicine, Detroit, MI 48201

[2]Institute of Environmental Health Sciences, Wayne State University, Detroit, MI 48201

Abstract

We previously reported that a low-level of lysosomal photodamage potentiated the phototoxic effect of subsequent mitochondrial photodamage mediated by the benzoporphyrin derivative BPD in murine hepatoma 1c1c7 cells. This was attributed to release of Ca^{2+} from damaged lysosomes and a calpain-mediated conversion of the autophagy-related protein ATG5 to a pro-apoptotic fragment. We now report a comparison of these results with those obtained with the human non small-cell lung cancer A549 cell line. A549 cells contained lower levels of ATG5 and were less responsive than 1c1c7 cultures to the PDT combination. A rapid appearance of caspase 3/7 activation together with formation of condensed chromatin indicated initiation of apoptosis in both cell lines, but to a lesser extent in A549 cultures. Both cell lines became highly vacuolated within 16 h of combination PDT or an equivalent phototoxic dose from BPD alone. The vacuole periphery was labeled with a fluorescent probe for the endoplasmic reticulum (ER), and vacuole formation was prevented by presence of the protein synthesis inhibitor cycloheximide. These effects are characteristics of a caspase-independent death mode termed paraptosis previously associated with ER stress. These studies suggest that paraptosis may be a more frequent outcome of PDT than has hitherto been realized.

Graphical Abstract

Morphology of cell death in A549 (NSCLC) cells during apoptosis (left) and paraptosis (right).

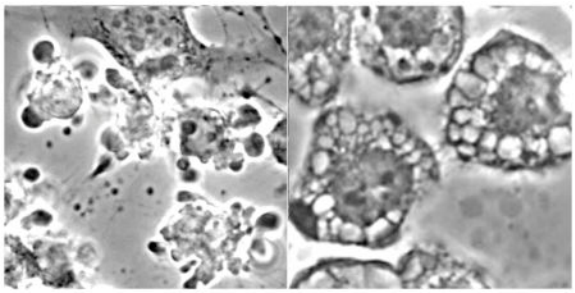

[*]Corresponding author's: dhkessel@med.wayne.edu (David Kessel).

INTRODUCTION

In 1996, Cincotta *et al.* reported that a sequential PDT protocol involving two photosensitizers could eradicate large (~1 cm depth) sarcomas in the mouse, something not feasible with either sensitizer alone (1). This combination utilized the phenothiazinium photosensitizer EtNBS along with benzoporphyrin derivative (Verteporfin, BPD). These photosensitizers preferentially target lysosomes and mitochondria, respectively (2,3). It was also found that photoactivation of EtNBS before BPD produced the optimal effect (1).

Cell culture studies provide evidence for a mechanism that can explain the above results. Simon's group had reported that ATG5, a protein involved in the assembly of autophagosomes, can be cleaved by calpain to form a proapoptotic truncated protein (i.e., tATG5) that can interact with mitochondrial membranes and sensitize them to subsequent damage by agents that trigger cytochrome c release (4). Using cultured murine hepatoma 1c1c7 cells, and the mitochondrial photosensitizer BPD and the lysosomal photosensitizer NPe6, we found that low level NPe6-induced lysosomal damage caused lysosomal Ca^{2+} release leading to cleavage of ATG5, a dramatic enhancement of BPD-mediated loss of mitochondrial membrane potential, and potentiation of cell killing (5–7). Knockdown studies demonstrated that the potentiating effects of prior lysosomal damage on BPD-mediated phototoxicity were ATG5 dependent (6).

PDT has a very limited role in the treatment of liver cancer but has an emerging use in the treatment of early stage non-small cell lung cancer (NSCLC). In this report we compare the effects of the combination PDT protocol on 1c1c7 and NSCLC A549 cells *in vitro*. The efficacy of the combination PDT protocol was slightly greater in 1c1c7 cells, which was consistent with its higher ATG5 content, greater loss of mitochondrial membrane potential, and higher caspase activities. A secondary result was observed upon examination of cell morphology 16 h after irradiation. Both cell lines exhibited a highly-vacuolated morphology which has characteristics consistent with a phenomenon termed paraptosis (8). Aside from one report (9), PDT had not hitherto been associated with paraptotic death.

MATERIALS AND METHODS

Chemicals and supplies

Lysosomal photodamage was created using the chlorin NPe6. It was obtained from Dr. Kevin M. Smith, Louisiana State University. BPD (benzoporphyrin derivative, Verteporfin) was used to initiate mitochondrial photodamage and was purchased from VWR (Cat No 1711461). Other reagents were obtained from Sigma-Aldrich and were of the highest available purity. Fluorescent probes used in this study were purchased from Life Technologies, Inc.

The antibody to ATG5 was provided by Abgent (San Diego, CA), Cat No AP1812A. This antibody is directed at amino acids 1–30 at the N-terminal of human ATG5 and cross-reacts with several other species including the mouse. The antibody was used at a 1:1000 dilution. The antibody to actin was provided by Cell Signaling Technology (Danvers, MA, Cat. No. 8456) and was directed at the carboxy-terminal region of human β-actin. This antibody

recognizes numerous isoforms including the murine protein. This was also used at a 1:1000 dilution.

Cell culture and clonogenic assays

Procedures for the growth of 1c1c7 cells have been described (10). A549 cells were obtained from the ATCC. Cell lines in use at this site are authenticated by the 'Biobanking and Correlative Sciences Core' of the Karmanos Cancer Institute. Both 1c1c7 and A549 cells were grown in RPMI1640 medium supplemented with 10% fetal bovine serum and antibiotics. Methodology for carrying out clonogenic assays has been described (10). To maintain pH in the absence of CO_2, irradiations were carried out in media buffered to pH 7.2 with HEPES. Colonies were stained with crystal violet and enumerated using an Oxford Optronix GelCount device. This device can identify groups of 30 or more cells as colonies. All experiments were performed in triplicate.

PDT protocols

Cells were cultured on 22 mm cover slips maintained in sterile plastic dishes. Cultures were incubated at 37°C with 20 μM NPe6 and/or 0.5 μM BPD for one h. The medium was replaced and the dishes were irradiated with a 600-watt quartz-halogen source. The light beam was passed through a 10 cm layer of water to remove IR and the bandwidth further confined by interference filters (Newport Crop, Irvine CA) to 660 ± 10 nm or 690 ± 10 nm to initiate photodamage catalyzed by NPe6 or BPD, respectively. The total light doses were initially 30 mJ/sq cm at 660 nm and 60 mJ/sq cm at 690 nm unless otherwise specified, so as to provide a comparison of effects of a similar PDT dose on both cell lines.

To test the effects of BPD alone, A549 cells were incubated with 0.5 μM BPD. After 1 h the medium was replaced and the dishes were given a light dose (690 nm) of 120 mJ/sq cm. This corresponds to an LD_{90} PDT dose, as determined in a colony formation assay. In some experiments the protein-synthesis inhibitor cycloheximide was added to culture dishes (0.5 μM) immediately after, or 4 h after irradiation.

Microscopy

Effects of photodamage on mitochondrial membrane potential ($\Delta\Psi_m$) were assessed by fluorescence microscopy using the probe MitoTracker Green (MTG) as previously described (5). The fluorescent probe ErTracker Green (ErTr) was used to visualize the endoplasmic reticulum (ER), or membrane derived from the ER. LysoTracker Green (LTG) was used to visualize late endosomes and lysosomes. Nuclear condensation and fragmentation effects were assessed using the fluorescent probe Hö33342 (11).

For colocalization analyses A549 cultures were incubated with 20 μM NPe6 or 0.5 μM BPD for 1 h at 37°C. ErTracker Green (ErTr), LTG, or MTG were present (as specified) during the final 15 min at a concentration of 500 nM. Fluorescent images were acquired using 360–420 nM excitation and a 650 nm high-pass filter in the light path (BPD, NPe6), or with 440–500 nm excitation and a 650 low-pass filter in the light path (LTG, MTG, ErTr). Images were acquired with a Nikon E-600 microscope using a Rolera EM-CCD camera and MetaMorph software (Molecular Devices, Sunnyvale CA). Phase contrast images were also

obtained. At least 3 images were acquired for each sample, with typical representations shown here.

DEVDase assays

Cells were collected 2 h after irradiation and assayed for DEVDase activity as previously described (10). This procedure monitors activation of caspases 3/7, an index of apoptosis. A kit provided by Life Technologies was used for this purpose (cat. no. E13184). Caspase activity is reported as nmol product/min/mg protein. Each assay was performed in triplicate. The Micro Lowry assay, using bovine serum albumin as the standard, was used to determine protein concentrations.

RESULTS

Photokilling by PDT combinations

A549 and 1c1c7 cultures incubated with NPe6 and BPD for one h, and then irradiated at 660 nm followed by 690 nm, exhibited levels of photokilling greater than what would have been predicted by a strictly additive effect (Fig. 1). With identical photosensitizer concentrations and light doses, the combination protocol was slightly less lethal to A549 cells (Fig. 1a) than to 1c1c7 cells (Fig. 1b). Previous studies with 1c1c7 cells, in which ATG5 was depleted, showed that the efficacy of the combinational PDT protocol correlated positively with ATG5 content (6). Western blot analysis indicated that A549 cells expressed considerably less ATG5 than 1c1c7 cells (Fig. 2).

Effects on mitochondrial membrane potential $\Delta\Psi_m$ and caspase activation

The irradiation protocol described in the legend to Fig. 1 had little, or no effect, on the $\Delta\Psi_m$ of 1c1c7 (Fig. 3a–c) or A549 (Fig. 3e–g) cultures that had been sensitized with only BPD or NP36. However, when the photosensitizers were used in combination, irradiation resulted in a rapid loss of $\Delta\Psi_m$ in 1c1c7 cultures (Fig. 3a vs. 3d), but not A549 cultures (Fig. 3e vs. 3h). The combination protocol did lead to an increase in DEVDase activity in both cell lines (Table 1). This measurement is usually taken as an index of procaspase 3/7 activation, proteases involved in the execution of the apoptotic program.

Morphologic effects of photodamage by the combination protocol

Morphological analyses of cultures 16 h after combinational PDT revealed numerous large cytosolic vacuoles in both A549 (Fig. 4a vs. e) and 1c1c7 (Fig. 4c vs. g) cells. Hö33342 staining of nuclei identified few, if any, cells in either untreated A549 (Fig 4b) or 1c1c7 (Fig. 4d) cultures with condensed chromatin (indicative of apoptosis). Cells with condensed chromatin were detected in both cell lines after the combination PDT protocol (Fig. 4f and h). Consistent with the DEVDase activation data, 1c1c7 cultures exhibited a greater percentage of cells with condensed chromatin. In both cell lines, the cells exhibiting the condensed chromatin exhibited a shrunken and rounded morphology rather than a flattened vacuolated morphology.

Evidence for paraptosis

Paraptosis is a mode of non-caspase-mediated cellular death. It is characterized by extensive cytoplasmic vacuolization, with the vacuoles derived from the ER and their formation inhibited by cycloheximide (8, 12–15). The fluorescent ER probe termed ErTr identified an extensive ER network in non-treated A549 cells (Fig. 5a,e). This network became condensed following combination PDT, and the periphery of the vacuoles was labeled with ErTr (Fig. 5b,f). Cotreatment of A549 cultures with 5 μM cycloheximide at the time of combinational PDT suppressed vacuole formation (Fig. 5c,g). The effect of cycloheximide was lost if it was added 4 h after irradiation (Fig. 4d,h). Similar results were obtained with 1c1c7 cells (unpublished data). Moreover, although cycloheximide suppressed vacuole formation, it neither promoted pro-caspase activation, nor restored colony formation to control levels (unpublished data).

Is the initiation of paraptosis elicited only by the combination PDT protocol? To examine this possibility, we exposed A549 and 1c1c7 cells to an LD_{90} PDT dose with BPD alone This provided a level of photokilling comparable to the combination PDT protocol, and resulted in pronounced vacuolization in both cell lines (Fig. 6a,b). Further analyses of A549 cells revealed that the vacuoles that formed using BPD LD_{90} PDT conditions (Fig. 7a vs. b) were also labeled with ErTr (Fig. 7c) and their formation was inhibited by cycloheximide (Fig. 7d).

Localization of photosensitizing agents

Consistent with a previous report involving 1c1c7 cells (11), fluorescence microscopy indicated that NPe6 (Fig. 8a) and LTG (Fig. 8b) fluorescence were punctate and highly colocalized in A549 cells (Fig. 8c). In contrast, BPD fluorescence was diffuse but accented with many puncta in A549 cells (Fig. 8d,g,j). Both LTG and MTG were primarily restricted to fluorescent puncta (Fig. 8e and h, respectively), while ErTr fluorescence was much more fibrous and diffuse (Fig. 8k). BPD and MTG fluorescence were high colocalized (Fig. 8i), as were also BPD and ErTr fluorescence (Fig. 8l). There also appeared to be some colocalization of BPD and LTG Fig. 8f) but this may be an artefact of the imaging procedure with some out-of-focus red pixels interfering with the green (LTG) pixels.

DISCUSSION

Previous studies with 1c1c7 cells have shown that low level photodamage to lysosomes markedly potentiates cell killing by subsequent photodamage to mitochondria (5–7). The enhanced photokilling produced by this protocol is initiated by the release of Ca^{2+} from photodamaged lysosomes, which activates calpain, leading to a calpain-mediated cleavage of ATG5 to form a pro-apoptotic fragment termed tATG5. As characterized by Simon's group (4), tATG5 can bind to mitochondria and sensitize the organelle to subsequent agents/treatments (such as BPD-induced photodamage to mitochondria) that can potentially activate the intrinsic apoptotic pathway. Knockdown studies in 1c1c7 cells clearly demonstrated that the efficacy of the combination protocol was related to ATG5 content (6).

As in 1c1c7 cells, a low level of lysosomal photodamage markedly potentiated the killing of A549 cells by subsequent photodamage mediated by BPD. Using identical treatment conditions, A549 cells were slightly, but consistently less sensitive (as scored in colony formation assays) than 1c1c7 cells to the combination PDT protocol. The reduced photokilling of A549 cells by the PDT combination may reflect differences in the ATG5 content of the two cells lines. This would be consistent with the proposal that tATG5 formation contributes to the greater-than additive effect of the combination.

Paraptosis is a term initially coined to define a striking morphological phenotype that was associated with non-caspase-mediated cell death (8). Three parameters appear to characterize paraptosis: 1) extensive accumulation in the cytosol of exceptionally large vacuoles, 2) labeling of these vacuoles with ER markers, and 3) vacuole formation is suppressed by the protein-synthesis inhibitor cycloheximide (8). These criteria appear to be present in both cell lines following either combination or BPD-only PDT, provided the treatment conditions are sufficient to provoke a high degree of photokilling. Although paraptosis is described as a death mode (8, 12–15), and the inclusion of cycloheximide suppressed the development of vacuoles in our studies, it did not rescue the cells from subsequent death. This likely reflects the cytotoxicity of cycloheximide itself. We cannot yet estimate the extent to which paraptosis contributes to PDT-mediated cell death.

With the exception of this study, we know of only one other report in which PDT was associated with an induction of paraptosis. That study employed a photosensitizer that caused direct nuclear photodamage (9). In that study it was reported that cells accumulating at the G_2/M interface underwent paraptosis while cells blocked from entering mitosis died via apoptosis (9). Although we cannot comment on any cell cycle- related connection in our study, results of our study and that of Pierroz et al. (9) raise the issue of how common paraptosis may be as a consequence of photodamage. Preliminary studies involving a variety of tumor cell lines of various lineages indicate that paraptosis is often observed, providing the PDT protocol causes a strong cytotoxic response.

Existing literature suggests that paraptosis is associated with ER stress (8,12–15). In this context, it is noteworthy that BPD fluorescence is colocalized with markers for both mitochondria and the ER (Fig. 8). Whether the BPD PDT-mediated induction of paraptosis in our studies reflects ER damage is unclear. It also remains to be established whether paraptosis is also detected after PDT *in vivo*, i.e., in animal tumor models and in the clinic. Studies in cell culture allow delineation of effects of photodamage resulting in direct photokilling, but do not permit the assessment of other effects relating to vascular shut-down or alteration in the immunologic response to cancer. With regard to the improved efficacy of the combination protocol, this may depend on the intrinsic level of ATG5 expression in a tumor population. The role of paraptosis in cancer control remains to be established. It may be a more common response to PDT than has hitherto been realized.

Acknowledgments

Partly supported by grant CA 23378 from the NIH and by a grant from the Office of the VP for research, Wayne State University. We thank Ann Marie Santiago for excellent technical assistance.

References

1. Cincotta L, Szeto D, Lampros E, Hasan T, Cincotta AH. Benzophenothiazine and benzoporphyrin derivative combination phototherapy effectively eradicates large murine sarcomas. Photochem Photobiol. 1996; 63:229–237. [PubMed: 8657737]
2. Peng TI, Chang CJ, Guo MJ, Wang YH, Yu JS, Wu HY, Jou MJ. Mitochondrion-targeted photosensitizer enhances the photodynamic effect-induced mitochondrial dysfunction and apoptosis. Ann N Y Acad Sci. 2005; 1042:419–428. [PubMed: 15965088]
3. Harvey EH, Webber J, Kessel D, Fromm D. Killing tumor cells: the effect of photodynamic therapy using mono-L-aspartyl chlorine and NS-398. Am J Surg. 2005; 189:302–305. [PubMed: 15792755]
4. Yousefi S, Perozzo R, Schmid I, Ziemiecki A, Schaffner T, Scapozza L, Brunner T, Simon HU. Calpain-mediated cleavage of ATG5 switches autophagy to apoptosis. Nat Cell Biol. 2006; 8:1124–1132. [PubMed: 16998475]
5. Kessel D, Reiners JJ Jr. Enhanced efficacy of photodynamic therapy via a sequential targeting protocol. Photochem Photobiol. 2014; 90:889–895. [PubMed: 24617972]
6. Kessel D, Reiners JJ Jr. Promotion of proapoptotic signals by lysosomal photodamage. Photochem Photobiol. 2015; 91:931–936. [PubMed: 25873082]
7. Kessel D, Evans CL. Promotion of Pro-Apoptotic Signals by Lysosomal Photodamage: Mechanistic Aspects and Influence of Autophagy. Photochem Photobiol. 2016; 92:620–623. [PubMed: 27096545]
8. Sperandio S, Poksay KS, Schilling B, Crippen D, Gibson BWNS, Bredesen DE. Identification of new modulators and protein alterations in non-apoptotic programmed cell death. J Cell Biochem. 2010; 111:1401–1412. [PubMed: 20830744]
9. Pierroz V, Rubbiani R, Gentili C, Patra M, Mari C, Gasser G, Ferrari S. Dual mode of cell death upon the photo-irradiation of a RuII polypyridyl complex in interphase or mitosis. Chem Sci. 2016; 16:6115–6124.
10. Andrzejak M, Price M, Kessel DH. Apoptotic and autophagic responses to photodynamic therapy in 1c1c7 murine hepatoma cells. Autophagy. 2011; 7:979–984. [PubMed: 21555918]
11. Reiners JJ Jr, Caruso JA, Mathieu P, Chelladurai B, Yin XM, Kessel D. Release of cytochrome c and activation of pro-caspase-9 following lysosomal photodamage involves Bid cleavage. Cell Death Differ. 2002; 9:934–944. [PubMed: 12181744]
12. Ghosh K, De S, Das S, Mukherjee S, Bandyopadhyay SS. Withaferin A induces ROS-mediated paraptosis in human breast cancer cell-lines MCF-7 and MDA-MB-231. PLoS One. 2016; 11:e0168488. [PubMed: 28033383]
13. Diederich M, Cerella C. Non-canonical programmed cell death mechanisms triggered by natural compounds. Semin Cancer Biol. 2016; 40–41:4–34.
14. Zheng H, Dong Y, Li L, Sun B, Liu L, Yuan H, Lou H. Novel benzo[a]quinolizidine analogs induce cancer cell death through paraptosis and apoptosis. J Med Chem. 2016; 59:5063–5076. [PubMed: 27077446]
15. Sugimori N, Espinoza JL, Trung LQ, Takami A, Kondo Y, An DT, Sasaki M, Wakayama T, Nakao S. Paraptosis cell death induction by the thiamine analog benfotiamine in leukemia cells. PLoS One. 2015; 10:e0120709. [PubMed: 25849583]

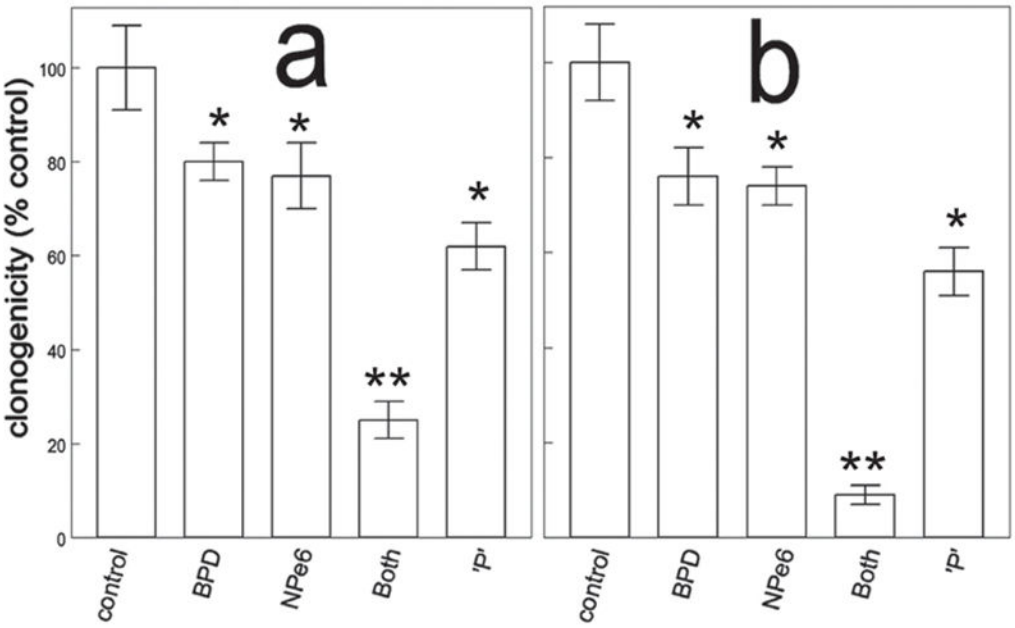

Figure 1.

Colony formation by A549 (a) and 1c1c7 (b) cells after low dose NPe6 PDT followed by low dose BPD PDT. Light doses were 30 mJ/sq cm (660 nm) for NPe6 followed by 60 mJ/sq cm (690 nm) for BPD. 'P' represents the predicted level of photokilling if effects were additive. Data represent mean ± SD for three separate experiments. Symbols: *, significantly different from controls ($p < 0.05$); **, $p < 0.01$.

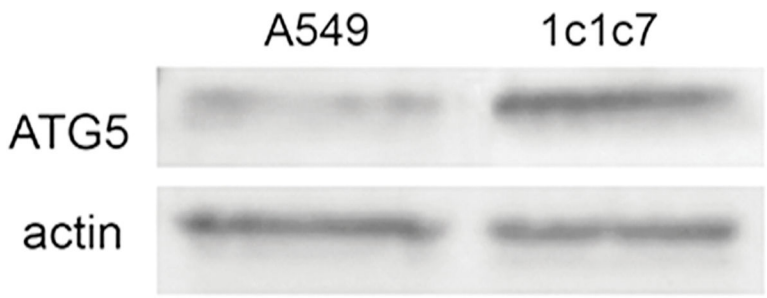

Figure 2.
Western blot analysis of ATG5 and actin in whole cell lysates of untreated A549 and 1c1c7 cells.

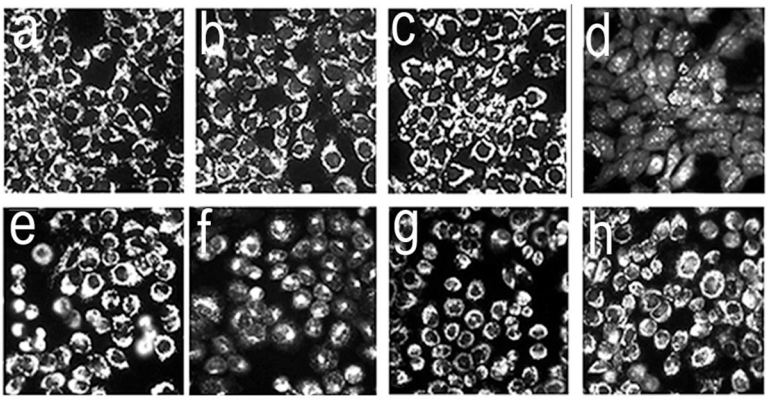

Figure 3.

Effects of individual photosensitizers and the sequential PDT protocol on $\Delta\Psi_m$ in 1c1c7 (a–d) and A549 (e–h) cells. Light doses are described in the legend to Fig. 1. Fluorescent probe, MTO (sensitive to the mitochondrial membrane potential). Images were acquired directly after irradiation. These represent typical results from three independent experiments. Panels: a,e = controls; b,f = BPD PDT; c,g = NPe6 PDT alone; d,h = NPe6 PDT followed by BPD PDT.

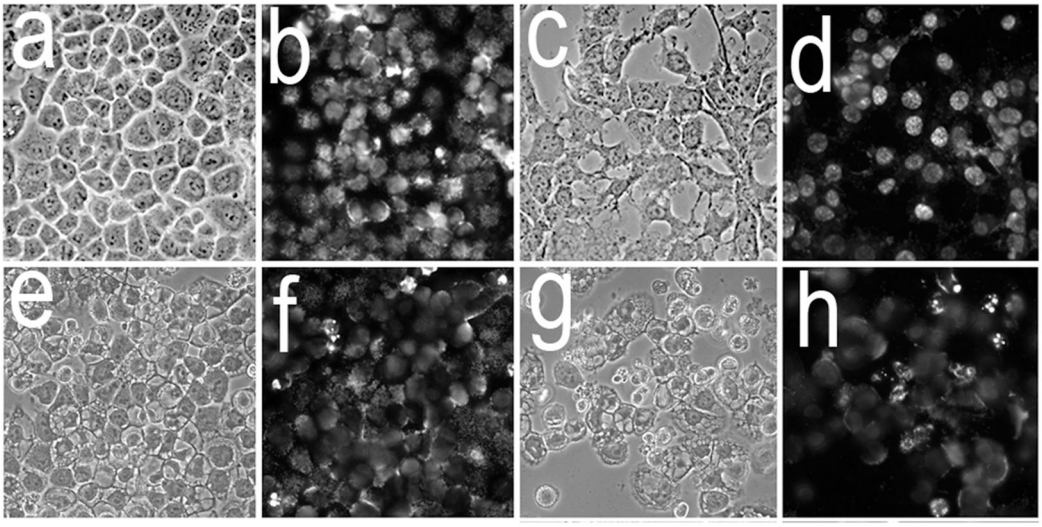

Figure 4.

Morphology and chromatin staining of A549 (a,b,e,f) and 1c1c7 (c,d,g,h) cells initially (a–d) and 16 h (e–h) after the combination PDT protocol. With the PDT conditions used, the clonogenic survival of A549 and 1c1c7 cells was ~20% and 10%, respectively. Phase contrast images (a,c,e,g) and Hö33342 fluorescence (b,d,f,h) are shown.

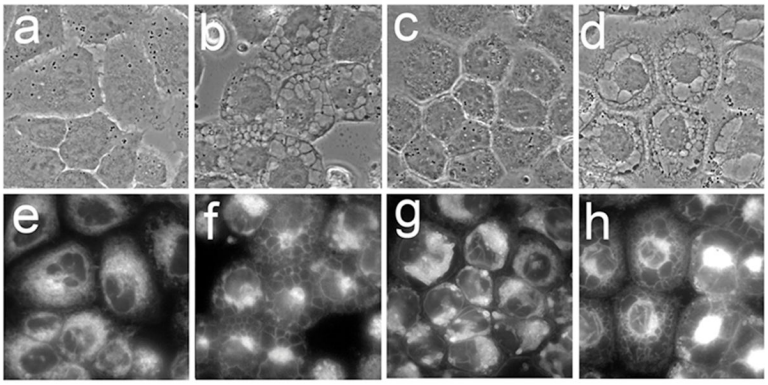

Figure 5.

Effects of cycloheximide on vacuole formation in A549 cells induced by combination PDT (LD_{90} conditions). Phase contrast (a–d) and ErTr fluorescence (e–h) images were acquired either prior to treatment (a,e) or 16 h after irradiation (b–d, f–h). Treatments were: a,d = untreated controls; b,e = combination PDT; c,f = combination PDT + 0.5 μM cycloheximide added just before irradiation; d,h combination PDT with cycloheximide added 4 h after irradiation.

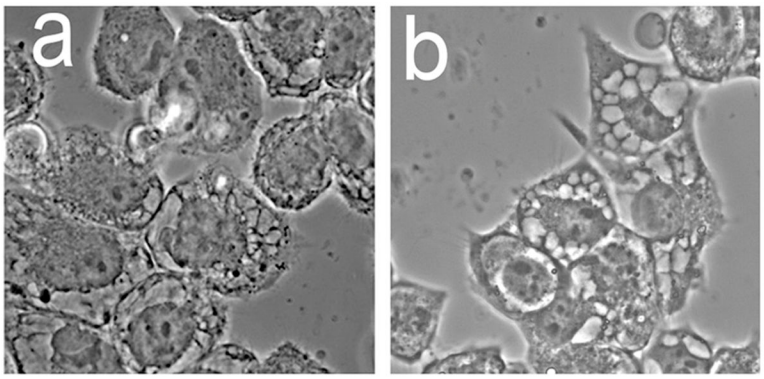

Figure 6.
Phase-contrast images of A549 (a) and 1c1c7 (b) cells 16 h after an LD_{90} PDT dose with BPD as sensitizer.

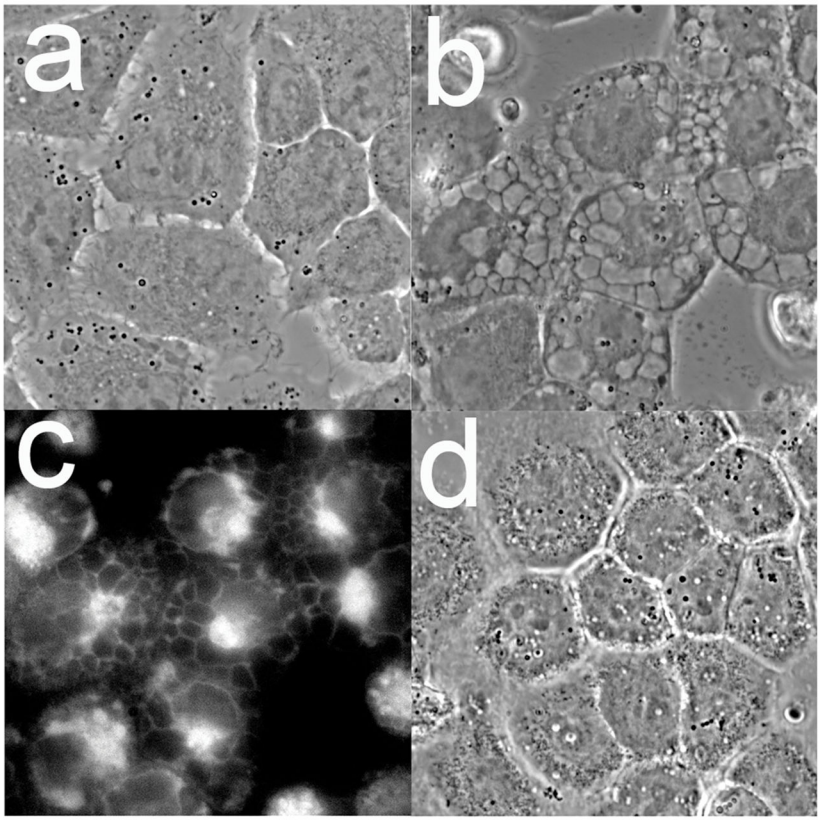

Figure 7.

Induction of paraptosis in A549 cells by BPD PDT. Panels are: (a) control cultures; (b) vacuoles formed 16 h after LD_{90} PDT conditions with BPD; (c) ErTr fluorescence of cells in panel b; (d) cell morphology 16 h after PDT with BPD in cultures in the presence of 5 μM cycloheximide.

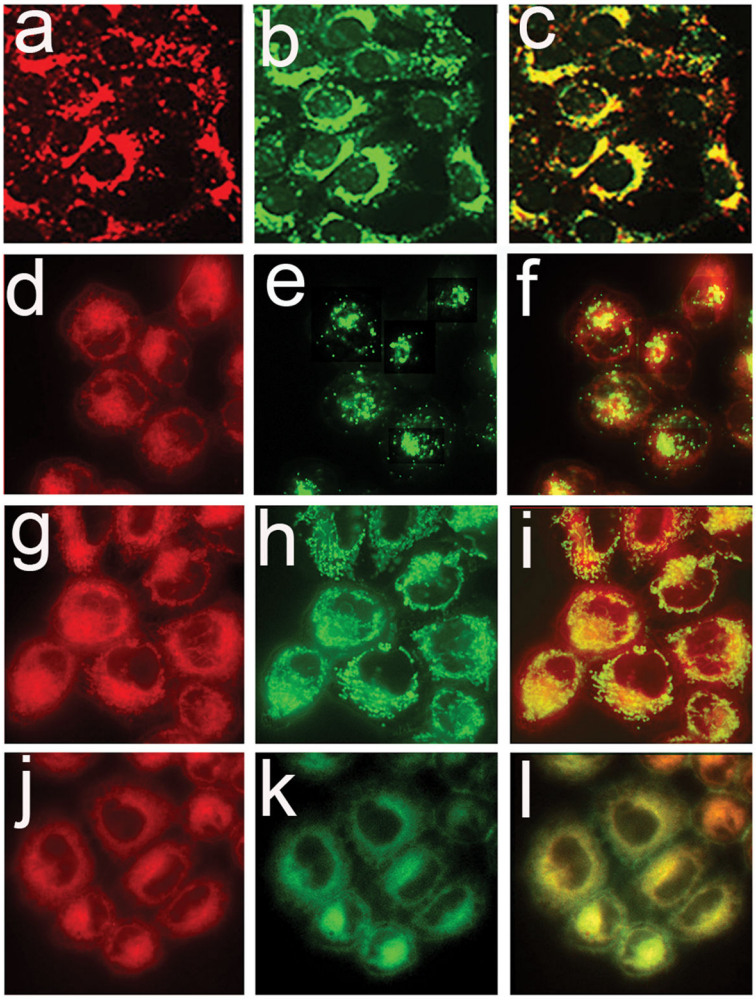

Figure 8.

Colocalization of NPe6 (top row) or BPD (bottom 3 rows) with fluorescent markers for lysosomes (top two rows), mitochondria (third row) and ER (bottom row) in A549 cell cultures. Cells were loaded with 20 μM NPe6 (a–c) or 0.5 μM BPD (d–l) for 1 h before imaging. Fluorescent probes for identification of lysosomes (LTG), mitochondria (MTG), and endoplasmic reticulum (ErTr) were added 15 min prior to imaging. Images for NPe6 (a) and BPD (d,g,j) fluorescence are shown along with fluorescence of LTG (b and e), MTG (h) and ErTr (k). Overlays of photosensitizer and probe fluorescence are shown in panels c,f,i and l.

Table 1

DEVDase activity associated with photodamage

Conditions	DEVDase activity	
	1c1c7	A549
control	0.07 ± 0.01	0.02 ± 0.01
BPD alone	0.21 ± 0.04	0.11 ± 0.01
NPe6 alone	0.11 ± 0.03	0.07 ± 0.02
BPD → NPe6	2.6 ± 0.15 *	0.53 ± 0.04 *

Cell cultures were treated with 20 μM NPe6 and 0.5 μM BPD for 1 h, before irradiation designed to produce LD_{90} level of photokilling using the two-sensitizer combination. DEVDase activity was measured 2 h after irradiation. DEVDase units = nmol product/min/mg protein. Values represent mean ± SD for three determinations.

* = statistically different from control values ($P < 0.05$).